MATERIALE PLASTICE
https://revmaterialeplastice.ro
https://doi.org/10.37358/Mat.Plast.1964

Experimental and Numerical Analysis of the Stress State Produced by a Circular Hole Concentrator

CONSTANTIN STOCHIOIU[1], VICTOR-MARIAN MARINESCU[2], EMILIA GEORGIANA OPRISAN[2], MIRUNA CIOLCA[1*]

[1]University Politehnica of Bucharest, Faculty of Industrial Engineering and Robotics, Department of Strength of Materials, 313 Splaiul Independenței, 060042, Bucharest, Romania

[2]University Politehnica of Bucharest, Faculty of Industrial Engineering and Robotics, 313 Splaiul Independenței, 060042, Bucharest, Romania

Abstract: *The paper proposes the analysis of strain and stress state, through experimental and numerical means, of a circular hole type concentrator. The strain state is analyzed through the microscopic Digital Image Correlation technique, due to the small scale of the samples, whose calibrated region is 10x8 mm. The numerical analysis is conducted using the Finite Element Method, through a static structural analysis, using a linear-elastic material model. The results from the two procedures are compared by means of strain field distribution around the stress concentrator and stress variation at the concentrator peak cross section. For validation, the analytical gross stress concentrator of the problem is used as baseline, K_{tg}. The results show that accurate reading can be achieved on this small scale. Additionally, the experimental method has also successfully identified crack initiations and propagations on the tested samples, significantly smaller than 1 mm, which can reveal future fracture mechanics analysis and supply data to models adapted to microscopic scale phenomena.*

Keywords: *stress concentrator, experimental analysis, FEM, microDIC*

1. Introduction

Stress concentrators are areas of a structural component where the geometry suffers sudden shifts. This entails, when a load is applied, an amplification of the stress and strain level in the vicinity of the stress concentrator, which often results in overloads and hotspots for failure of the component [1]. These shape variations are often functionally important and cannot be avoided making it necessary to study them in detail to establish useful practical conclusions about the effective ways of modeling these elements. Examples of stress concentrators are keyways, joints, threads, holes etc. The latter is of high importance in structural design, especially the circular hole, as it is inevitable when assembly is required with bolts or rivets [2], but is also, due to its geometric simplicity, used for simulating simple defects or as reference for developing more complex models [3-6].

In terms of experimental analysis of stress concentration, it is often more accessible to follow the effects on the strain distribution, as strain can be determined through non-contact means [7]. One such method is the Digital Image Correlation (DIC), a technique used to determine the shifts of a speckle pattern applied on the surface of the analyzed component [8]. These shifts in the speckle pattern are directly linked to the strain state on the component's surface. Stress state can indirectly be calculated if the stress-strain relation of the material is known. The DIC method has proven highly efficient in determining strain field distributions in numerous applications such as medical [7, 9], material testing [8, 10], vibration analysis [11] or stress concentration effects [12]. Recently, the DIC method has been developed to encompass small scale component analysis as well, by employing it along with a microscope [13].

For stress state determination, the most often used method is the Finite Element Analysis (FEA). It is often employed to model complex geometries or load cases and has become a pillar in mechanical engineering design [14]. It, however, has the shortcoming of requiring experimental validation.

**email: miruna.ciolca@upb.ro*

By coupling the two methods, one can successfully characterize both the stress and strain state of a geometry containing stress concentrators and can contribute to the improvement of a given structure.

In the present work, the stress concentration effects of a circular hole in a thin finite plate have been chosen for study, in samples of small dimensions, requiring microscopic analysis. The material was chosen with a simple, linear elastic stress-strain relation, allowing the implementation of Hooke's general law. Through microDIC analysis, the experimental strain distribution was analyzed, to determine the method's capabilities on such small-scale components, along with the identification of other localized effects. Supplementary, the stress concentrator effects of this type of geometry have an analytical solution [15], which was used to validate the two methods.

2. Materials and methods

The stress concentration effects were analyzed through experimental investigations, on samples fabricated from an isotropic linear-elastic polymer, and numerical analysis through the finite element method, using the same geometry as for the experimental part. The analysis followed the comparison between experimental and numerical results, regarding strain distribution on the sample calibrated area as well as the strain and stress distribution in the concentrator peak cross-section.

2.1. Experimental investigations

The material chosen was a clear Poly Methyl Methacrylate (PMMA), supplied as a 1 mm thick sheet. It is a highly versatile thermoplastic polymer, which has exhibited brittle, linear-elastic behavior up to failure. Two types of experiments were carried out: tensile tests to failure, to determine the mechanical properties of the material and tensile tests on samples with a stress concentrator, to evaluate its effect on the geometry.

From the PMMA sheets, multiple samples were laser cut, with the geometry specified in Figure 1. Three specimens were used for the mechanical characterization and five specimens for the analysis of the stress concentrator effects. The samples were measured in the calibrated regions, as the geometry suffered slight alterations in dimensions due to the laser beam diameter. The most notable disparity is the center hole, whose diameter was measured at approximately 4.3 mm instead of 4 mm.

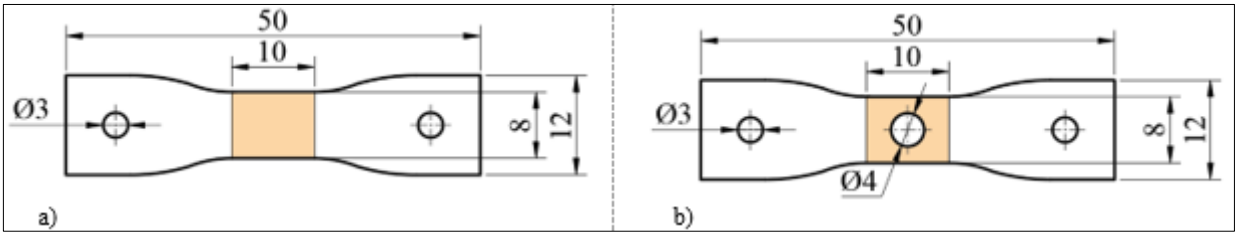

Figure 1. Dimensions of the tested samples, orange denoting the calibrated region:
a) for tensile testing; b) for stress concentrator analysis

Strain measurement was achieved with the Digital Image Correlation technique, using a Dantec Dynamics Q400 system, with a sampling frequency of 2 Hz. Due to the small size of the samples, the DIC equipment was mounted on a Leica M125 optic microscope, allowing a maximum recordable area of 10x10 mm. Loading for the mechanical characterization and stress concentrators analysis was performed with a miniature tensile testing machine. It was designed particularly for this type of research, adapted for the sample sizes and the microscope, as the specimen dimensions dictated the testing equipment dimensions. The testing machine used a pair of twin lead screws which, when turned by the stepper motor, moved the two jaws in opposite directions to maintain the calibrated region of the sample in the imaging area. Testing was done for both batches with a loading speed of 1 mm/min. The applied load was measured using a HBM U9C 1 kN force transducer, mounted in series with the tested sample. The testing equipment is presented in Figure 2.

A stochastic pattern consisting of a white background with black speckles was applied to the samples, using an aerograph capable of producing appropriate speckle size for microscopy.

Post processing of the data obtained from the deformation was conducted with the ISTRA4D image correlation software.

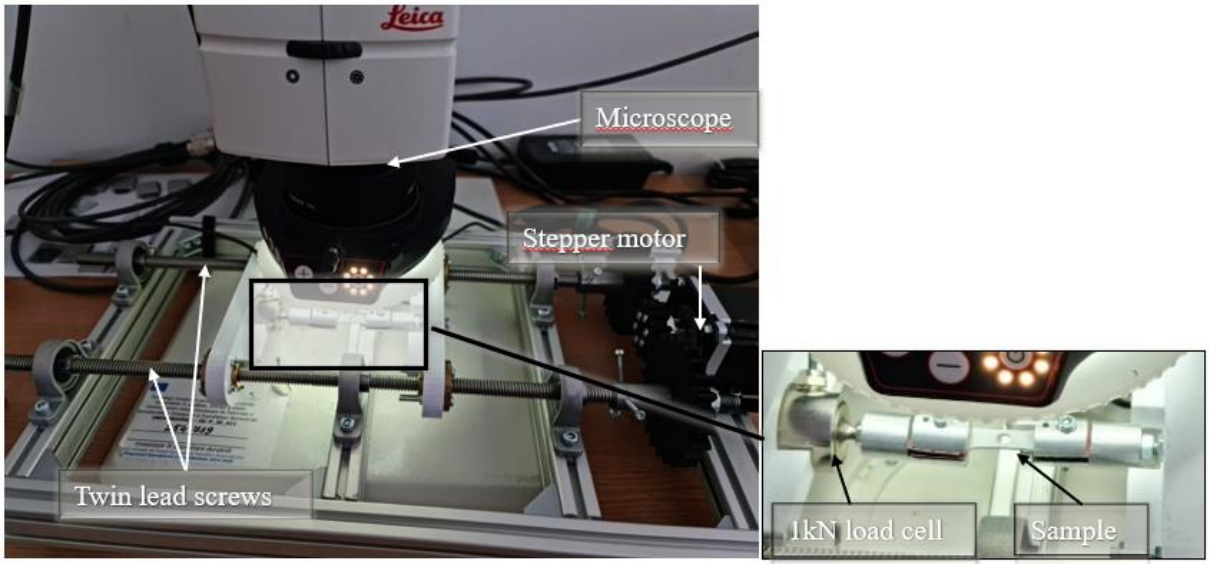

Figure 2. Testing equipment

2.2. Numerical investigation

The numerical analysis was carried out using Ansys' Static Structural module. The PMMA material was created in Engineering Data, implementing a linear elastic model, using the Young modulus and Poisson ratio obtained in the mechanical characterization. The geometry was designed in AutoCAD, following the dimensions in Figure 1b and imported into the analysis (Figure 3a). An adjustment was necessary to increase the diameter of the center hole to 4.3 mm. Furthermore, the geometry was split in two, to allow the extraction of numerical results on the Path which follows the concentrator's peak cross-section (Figure 3b).

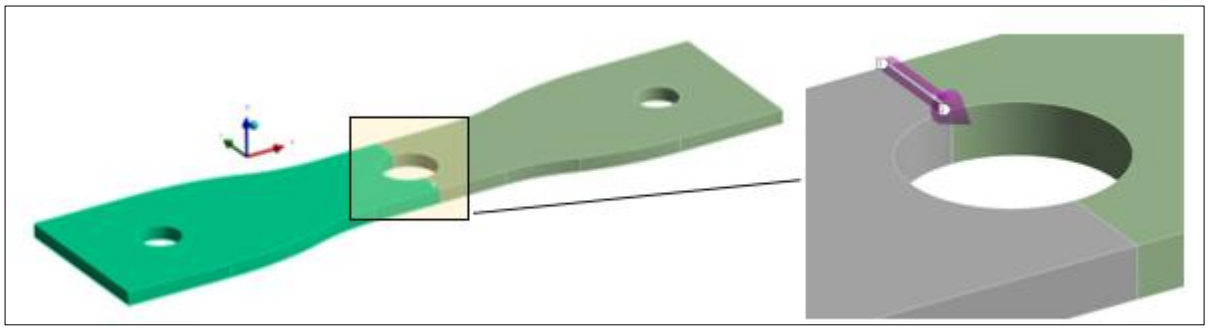

a b

Figure 3. FEM Geometry: a) stress concentrator sample; b) detail of the analyzed path

Meshing was performed using the Solid 185 element, imposing an element size of 0.5 mm and a division of 10 elements on the selected Path. The resulting mesh consisted of 6228 elements and 8940 nodes (Figure 4a). The boundary conditions were a fixed support on one end of the sample and a force on the opposite end (Figure 4b). The value of this force was correlated to the load level of the sample for which the stress concentrator effects were analyzed.

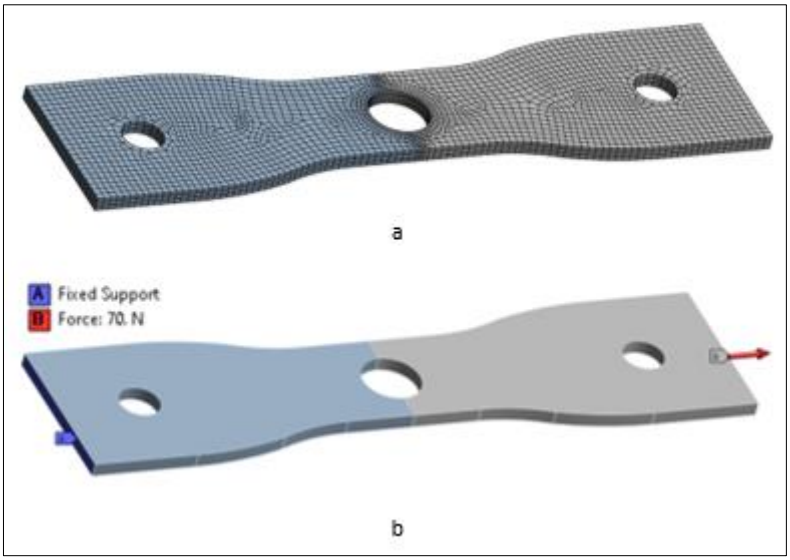

Figure 4. Finite element model: a) mesh; b) boundary conditions

3. Results and discussions

3.1. Mechanical characterization

Using the ISTRA 4D software, the interest area from the captured images has divided into facets, 55x55 pixels in size and distance of 51 pixels between the facets (Figure 5a). From the processed strain field data, the longitudinal and transverse strains have been extracted on the direction of load and perpendicular to it respectively, as average values on the calibrated area (Figure 5b), resulting in conventional values. The stress-strain curves obtained through tensile testing are presented in Figure 6a and the longitudinal strain versus transverse strain in Figure 6b. Young modulus, E, and Poisson's ratio, ν, have been calculated as the slopes of the curves in the 0.1-0.6 % longitudinal strain interval and are presented, along with ultimate stress, σ_u, and strain, ε_u, in Table 1.

.

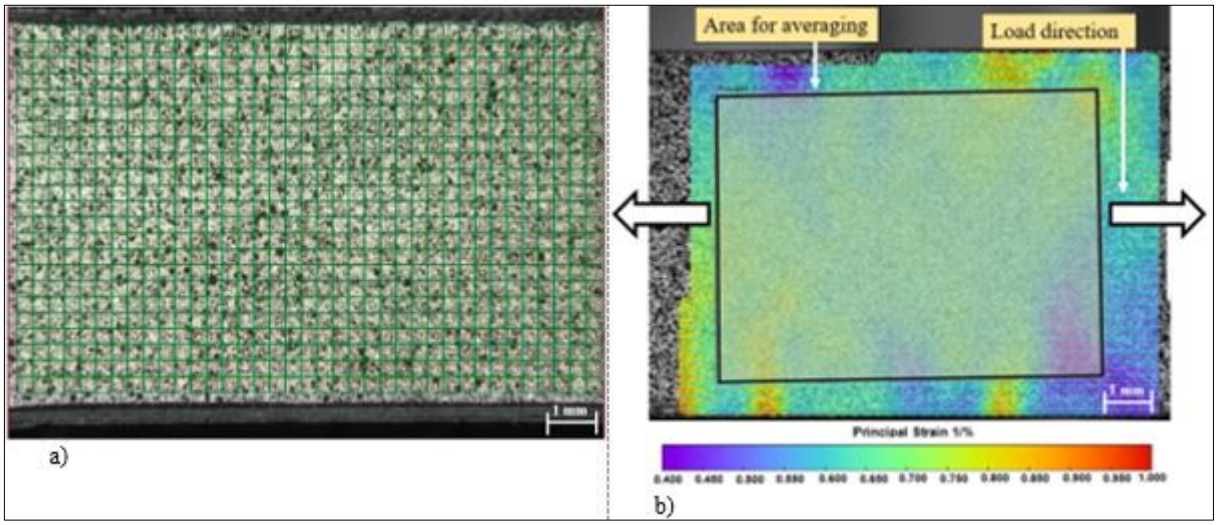

Figure 5. Digital image correlation processing: a) facets on the region of interest; b) example of strain field data, principal strain 1

Table 1. Mechanical properties of the tested PMMA samples

Property	Unit	Value
E	MPa	2546±91
ν	[-]	0.35±0.02
σ_u	[MPa]	23.76±4.04
ε_u	[%]	0.86±0.05

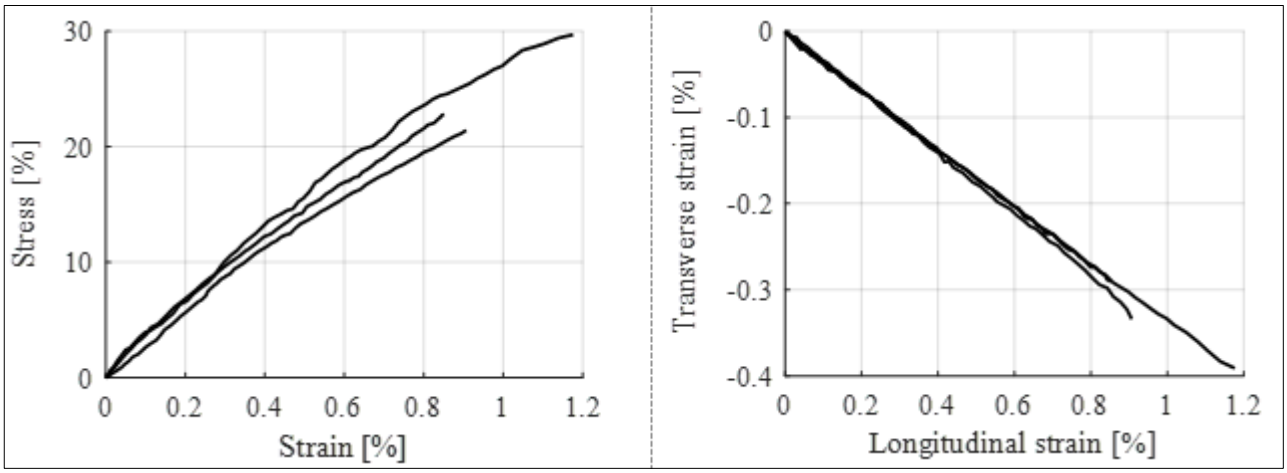

Figure 6. Mechanical characterization results: a) stress-strain curve;
b) longitudinal strain versus transverse strain

3.2. Stress concentrator analysis

The five tested samples are presented in Figure 7. All samples have failed in the vicinity of the stress concentrators. However, failure did not always occur at the peak of the stress concentrator or did not follow a path perpendicular to the load direction. For the first case, the notable example is for the sample denoted C4, where the crack initiated at a significant distance, on the outer contour, while for the latter case, sample C3, for which the cracks have propagated on a diagonal line from the center hole towards the extremities. This can be explained by microcracks forming during loading in other areas than the stress concentrator. This is a characteristic of the brittle behavior of the material, with some cases failure appearing by the propagation of these cracks towards the center hole.

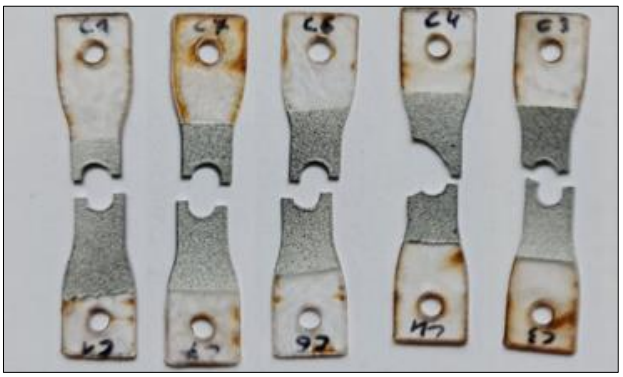

Figure 7. Samples with stress concentrator

The strain field processing was made with denser facets, 25x25 pixels in size and 21 pixels distance between them.

A representative principal strain distribution is presented in Figure 8a. The maximum strain is recorded at the stress concentrator peak, while the minimal values are positioned at 90° on the hole contour. In Figure 8b, sample C4 is detailed, where multiple cracks have been recorded before failure.

The figure was captured at a load level of 100 N. Of significance for this test is one crack, which was produced on the upper right edge of the sample, and propagated to become visible at approximately 73 N, with a size of approximately 0.6 mm. It continued increasing until producing failure of the sample, following the propagation of the crack initiated at that point. A second crack, smaller in size, became visible on the inferior portion of the circular hole, at approximately 97 N.

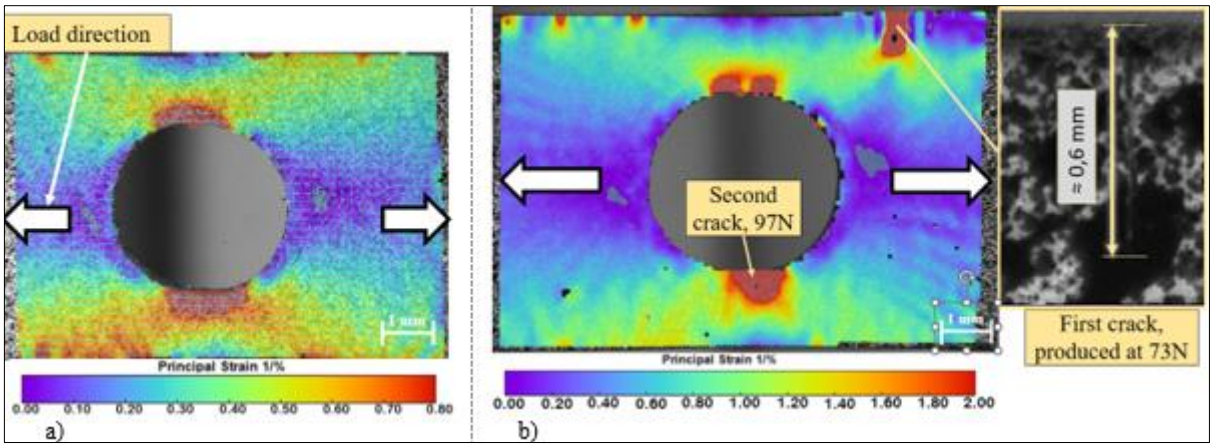

Figure 8. Principal strain field for stress concentrator samples: a) representative; b) sample C4 with crack propagation at 100 N load

The microcracks produced on the edge of the sample, while without such a high impact as for samples C4 and C3, have been recorded on all samples, as can be seen in Figure 8a as well. It is theorized that these cracks are produced due to the local accumulation of material during melting with the laser beam, which created non-uniformities in the geometry.

While it did not present a significant impact on the present work other than revealing localized hotspots, where failure risked occurring, it would be worth analyzing this effect separately. By adding a sanding stage in the fabrication process, with a high grit-size sandpaper the accumulation of material would be reduced or eliminated, while at the same time, not adding additional defects to nucleate cracks.

The stress concentrator effects produced by the circular hole are further analyzed, by extracting the major principal strain on lines near the concentrator peak, radiating from the hole (Figure 9) and calculating an average for the two lines per sample. The variation of this principal strain is extracted for the load of 70 N, which is sufficiently high to produce a clear strain field distribution, but low enough to avoid the appearance of cracks in the concentrator region.

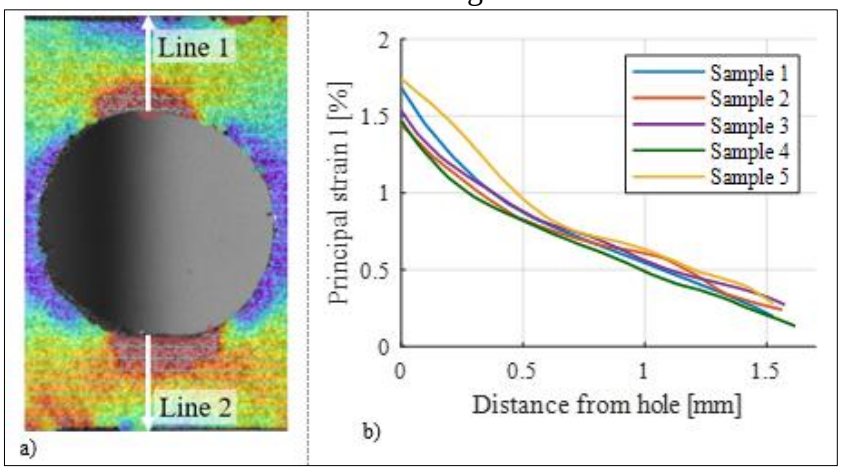

Figure 9. Maximum principal strains: a) paths for extraction; b) variation along the paths

A clear, repeatable variation can be noticed, with strain values ranging from 1.5-1.8% at the concentrator apogee, down to 0.2-0.3% at the sample outer contour.

From the presented experimental results, it can be extracted that the stress concentrator effects of small-scale parts can be successfully determined using the digital image correlation technique paired with a microscope and adapted loading equipment. The results have also revealed that, at high loads, additional effects appear, related to the failure mechanism of the material, which in the case of the chosen polymer, are brittle in nature. These failure mechanisms exceed the analysis of the present work but are worth following in the future, by taking into consideration elements of fracture mechanics.

3.3. Results of the numerical analysis

The numerical analysis was conducted also using a load of 70 N. The results of interest are those which allow a comparison with the experimental procedure: the strain distribution in the vicinity of the stress concentrator and the strain variation in the cross section at the concentrator apogee. Supplementary, the normal stress along the load direction, X in the present configuration, has been extracted, to calculate a stress concentration factor and to compare it with the analytical results available in the literature.

The maximum principal strain distribution in the concentrator vicinity is presented in Figure 10. The strain distribution shows that the highest value is in the concentrator apogee, at the circular hole contour level, with a decrease in value in the cross section, towards the extremity of the sample. These results are faithful to the experimental ones, presented in Figure 8. The notable difference between the two are the local effects of microcracks, which begin to form on the outer contour of the sample and can by the numerical model, which was limited to linear elasticity.

The variation of the major principal strain on the paths in the concentrator peak cross-section is extracted in Figure 10, along with the experimental results, for comparison. A good correlation can be observed in the concentrator vicinity and a slight numerical over-evaluation at the extremities, with values ranging from 1.50% at the concentrator apogee to 0.3% at the cross-section extremity.

In Figure 11a, the normal stress distribution in the load direction, the X axis is extracted. The stress state on the selected path has been extracted in Figure 11b, where the calculated experimental evolution has been added. The latter has been calculated using Hooke's general law, considering plane stress and the linear-elastic behavior of the material (1).

$$\sigma_X = \frac{E}{1-\nu^2}(\varepsilon_X + \nu\varepsilon_Y) \tag{1}$$

with ε_X, the recorded strain on the load direction and ε_Y, the recorded strain on the transverse direction.

The correlation between experimental and numerical results validated capability of the numerical model to reproduce the targeted phenomenon. This allowed further analysis of the stress concentrator, by calculating the gross stress concentration effect, K_{tg}, (2):

$$K_{tg} = \frac{\sigma_{max}}{\sigma} \tag{2}$$

where σ_{max} represents the maximum normal stress at the concentrator peak and σ, the gross normal stress:

$$\sigma = \frac{N}{A} \tag{3}$$

with N the load and A sample gross cross section, with no hole.

In the current configuration, the experimental analysis produced $K_{tg,Exp} = 4.86 \pm 0.22$ and the numerical analysis produced $K_{tg,FEM} = 4.47$. The analytical value calculated using the relation from [15] (Figure 12) produces, for the ratio d/H=0.54, a value of $K_{tg} = 4.61$.

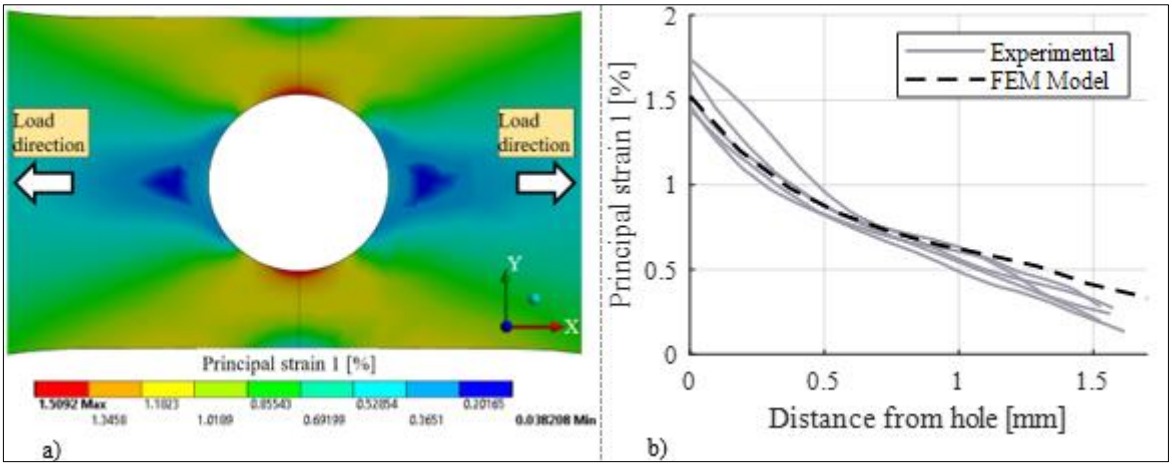

Figure 10. Major principal strain: a) distribution in the concentrator vicinity; b) variation on the path radiating from the concentrator

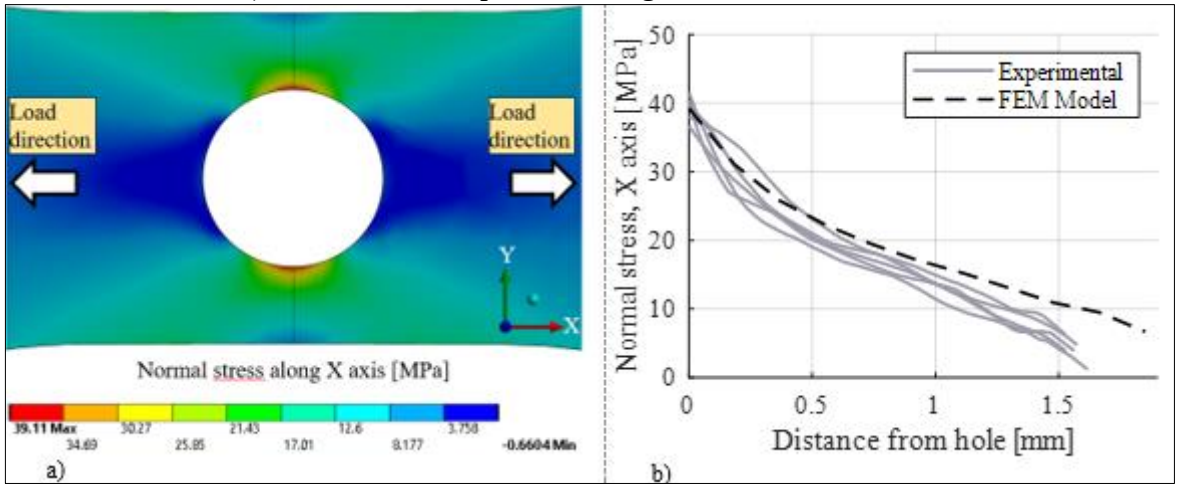

Figure 11. Normal stress along X axis: a) stress distribution; b) variation on path radiating from the center hole

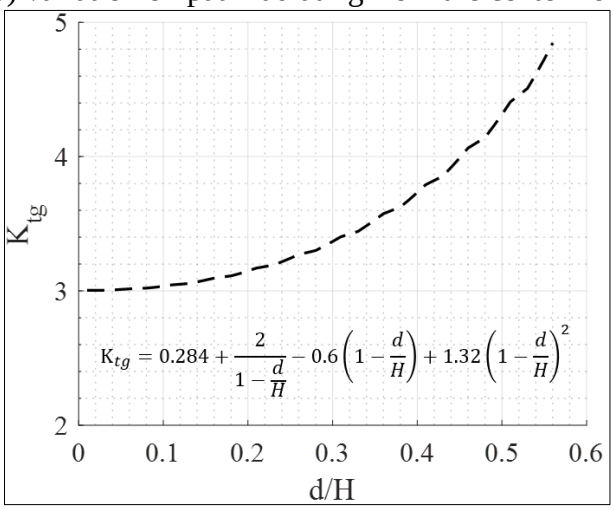

Figure 12. Variation of stress concentration effects for a center hole in a thin finite plate, reproduction from [15]

The good correlation between experimental and numerical stress concentration analysis proves the potential of the microDIC technique to analyze variable strain fields. Moreover, the technique can identify localized effects, such as microcracks, as has been the case in the present work. It has been

shown that at high loads, approaching failure, they tend to dominate the sample behavior under load. Numerical analysis using FEM routines requires, for this type of behavior, specific modeling and considering phenomena described by fracture mechanics. As future development of the presented work, crack propagation can be considered and modeled. This would require, firstly, a mechanical characterization of the crack propagation and the implementation of an adequate model.

4. Conclusions

In the current work an experimental and numerical analysis of the stress concentrator effect on a small-scale geometry, fabricated from a linear-elastic brittle material has been presented. The experimental analysis was conducted using the microDIC technique to determine the strain distribution around a circular hole in a thin plate with finite width.

The dimensions of the sample plates as well as the hole were such that a microscope would be required to accurately determine the strain effects produced.

A numerical model was constructed using the Finite Element Method in the linear-elastic domain. The model was used for comparison purposes with the experimental results, but also for the extraction of the stress state, which led to calculating the stress concentration factor.

A good correlation was found between experimental and numerical results along with the analytical one, represented by the gross stress concentration factor.

Moreover, the experimental results showed that the microDIC technique is highly capable of determining localized effects produced by cracks recorded during loading. These were all smaller than 1 mm in size before producing the brittle failure of the samples and appeared both at the hole level and on the outer contour of the sample.

Consequently, the capability of the microDIC technique can also be extended to determine localized effects such as the production and propagation of microcracks.

References

1. ATANASIU, C., SOROHAN, Ș., Stress concentration in the components of a drive coupling, Journal of Engineering Sciences and Innovation, **6**(3), 2021, 223–234.
2. MAIER, R., Study on increasing performances of hybrid composite through pull out compression test assessement, *Mater. Plast.*, **57**(1), 2020, 329–335.
3. HILL, H.N., Stress-Concentration Factors Around a Central Circular Hole in a Plate Loaded Through a Pin in the Hole, Photoelasticity, 1969, 159–170.
4.MARCU, F., Considerations on the Stresses Concentration Factor, Journal of Engineering Studies and Research, **18**(4), 2016, 47–52.
5. LIU, H., LIU, S., ZHAO, Y., WANG, J., ZHENG, C., XIA, Z., et al., Numerical simulation of the effect of internal hole defect size on the mechanical properties of limestone, PLoS ONE, **17**(10), 2022, 1–20.
6. YAN, Y., WEN, W.D., CHANG, F.K., SHYPRYKEVICH, P., Experimental study on clamping effects on the tensile strength of composite plates with a bolt-filled hole, Composites Part A: Applied Science and Manufacturing, **30**(10), 1999, 1215–1229.
7. NGUYEN, M.T., ALLAIN, J.M., GHARBI, H., DESCELIERS, C., SOIZE C., Experimental multiscale measurements for the mechanical identification of a cortical bone by digital image correlation, Journal of the Mechanical Behavior of Biomedical Materials, **63**, 2016, 125–133.
8. WANG, Y.H., JIANG, J.H., WANINTRUDAL, C., DU, C., ZHOU, D., SMITH, L.M., et al., Whole field sheet-metal tensile test using digital image correlation, Experimental Techniques, **34**(2), 2010, 54–59.
9. SZÁVA, D.T., BÖGÖZI, B., SZÁVA, I., TARCOLEA, M., COMANEANU, R.M., ORMENISAN, A., Plastic materials used in experimental investigations regarding dental implants biomechanics, *Mater. Plast*., **52**(2), 2015, 221–224.

10. CERBU, C., XU, D., WANG, H., ROȘCA, I.C., The use of Digital Image Correlation in determining the mechanical properties of materials, IOP Conference Series: Materials Science and Engineering, **399**(1), 2018.
11. HAGARA, M., TREBUŇA, F., HUŇADY, R., KALINA, M., SCHRÖTTER, M., Experimental identification of modal parameters of thin metal sheets by using of DIC, Procedia Engineering, 2012, **48**, 2012, 180–188.
12. MOHAMED MAKKI, M., CHOKRI, B., Experimental, analytical, and finite element study of stress concentration factors for composite materials, Journal of Composite Materials, **51**(11), 2017, 1583–1594.
13. RUSIN, T. KOPERNIK, M., Characterization of Biocompatible Materials Using Stereo Microscope 3D Digital Image Correlation, Advanced Engineering Materials, **18**(9), 2016, 1651–1660.
14. COMANICI, A.M., GOANTA, V., BARSANESCU, P.D., Theoretical and experimental study of specimens with stress concentrators in dependence of stress triaxiality, Ciencia e Tecnologia dos Materiais, **29**(1), 2017, 254–261.
15. PILKEY, W.D., PILKEY, D.F., Petersons Stress Concentration Factors- 3rd Edition, 2008.

Manuscript received: 21.08.2023